Robot-Assisted Individualized Medial Patellofemoral Ligament Reconstruction in Skeletally Immature Patients With Recurrent Patellar Dislocation

A Single-Center Retrospective Study

Qiuzhen Liang,* PhD, Chaofan Liao,* MASc, Zandong Zhao,* MASc, Junxuran Li,[†] MASc, Hongwei Zhan,* MASc, Peidong Liu,* MASc, Xin Kang,* MD, Bo Ren,* PhD, Bin Tian,* MD, Liang Zhang,*[‡] MD, and Jiang Zheng,*[‡] MD
Investigation performed at Sports Medicine Center, Honghui Hospital, Xi'an Jiaotong University, Xi'an, Shaanxi, China

Background: The surgical treatment of patellar instability in children and adolescents can be challenging, as successful surgical techniques used in adults may pose a risk to the open growth plate when applied in this younger population.

Purpose: To review a series of adolescent patients with recurrent patellar dislocation who underwent robot-assisted individualized medial patellofemoral ligament (MPFL) reconstruction.

Study Design: Case series; Level of evidence: 4.

Methods: This retrospective clinical study included 76 patients with recurrent patellar dislocation who underwent MPFL reconstruction by a robot-assisted technique or adductor magnus sling technique from June 2018 to August 2022. All patients were divided into the robot-assisted group (42 patients) or the adductor magnus sling group (34 patients). In both groups, a semitendinosus autograft was used for the MPFL reconstruction. In the robot-assisted group, the graft was fixed to the femur using an interference screw. In the adductor magnus sling group, the graft was loped around the adductor magnus. During the surgery, the distance between Schoettle point and the medial distal femoral physis, along with the simulated angle range of the bone tunnel and the optimal angle, was recorded in the robot-assisted group using an intraoperative 3-dimensional navigation system. The clinical results were evaluated using preoperative and postoperative functional scores and imaging.

Results: All patients returned for follow-up at a mean of 39.7 ± 9.8 months after surgery. The mean age of the patients was 13.3 years (range, 10-16 years). The Schoettle points were all located below the medial distal femoral physis, with a mean distance of 6.48 ± 1.78 mm from Schoettle points to the medial distal femoral physis. The angle range of the bone tunnel was achieved by targeting a mean of $8.6°$ to $23.4°$ anteriorly and $10.9°$ to $17.8°$ distally, with the optimal angles being $14.6°$ anteriorly and $13.5°$ distally. No patients experienced recurrent patellar instability after surgery; however, the functional scores in the robot-assisted group were slightly higher than those in the traditional adductor magnus sling group (International Knee Documentation Committee score: 93.2 ± 6.2 vs 86.1 ± 7.9; Lysholm score: 90.0 ± 8.1 vs 85.9 ± 7.3; Kujala score: 87.8 ± 6.8 vs 83.0 ± 8.8; all $P < .05$) at the last follow-up. All the patients had normal patellar tracking, except for 3 patients (8.8%) in the adductor magnus sling group. None of the patients exhibited subsequent growth deformity or any evidence of physeal invasion.

Conclusion: The intraoperative robotic navigation system confirmed that the Schoettle point can be safely positioned in patients with open epiphyses. The robot-assisted design of individualized anatomic reconstruction of the MPFL using a forward distal oblique bone tunnel is safe and effective, demonstrating good clinical outcomes.

The incidence of patellar dislocation ranges from 29 to 40 per 100,000 individuals, with the peak incidence of first-time dislocation occurring at age 15 years.[11] The surgical treatment of patellar instability in children and adolescents can be challenging yet rewarding.[1] The medial patellofemoral ligament (MPFL) serves as the primary medial static stabilizer,[12] and isolated MPFL reconstruction is the most prevalent and efficacious surgical intervention for patients lacking severe osseous deformities.[5] However, successful surgical techniques used in adults may endanger the open growth plate when used in children and adolescents. Few studies have reported the outcomes of these MPFL reconstruction techniques in skeletally immature patients.

It was previously believed that soft tissue surgeries such as primary repair, medial retinacular imbrication, cerclage suture fixation around the medial collateral ligament or adductor magnus insertion, the Roux-Goldthwait procedure, and other methods using soft tissue attachment on the femur to prevent the risk of femoral physis injury would be a more appropriate approach.[7,17,28] However, these methods of tendon fixation, which depend on soft tissue sutures, are not as sturdy as bone tunnel fixation. Additionally, conducting soft tissue surgery makes achieving anatomic repair of the MPFL challenging. Because it has been shown that, historically, operative procedures in children have a high failure rate, anatomic reconstruction of the MPFL has been advocated in skeletally immature patients as well.[19]

The MPFL lies within a sulcus between the medial femoral epicondyle and the adductor tubercle.[6] Some literature describes this location at the distal end of the femoral growth plate, approximately 4 to 16 mm, while some scholars have described extensions of the femoral attachment as being slightly proximal to the physis.[10,24,25] Farrow et al[8] has also demonstrated this relationship and emphasized the undulating nature of the distal femoral physis. Although still somewhat controversial, most references describe the MPFL origin footprint at or below the physis.[19,24]

The femoral insertion of the MPFL is typically located within a 5-mm area that is now widely known as the Schoettle point.[22] In the present study, the radiographic technique described by Schöttle et al[22] was used to identify the MPFL insertion and its relationship to the distal femoral physis. However, because of the complex physeal anatomy, consensus on the relationship between the MPFL insertion and the distal femoral physis has not been reached.[16,18]

The traditional surgical approach involves locating the Schoettle point on the standard lateral radiograph and then penetrating the guide to avoid the epiphysis, intercondylar notch, and distal femoral cartilage. This process often requires repeated puncture and fluoroscopy for surgeons in the early stages of their careers or those with a low volume of MPFL reconstruction cases in skeletally immature patients, to determine a specific angle that meets the aforementioned requirements. Although a small number of scholars have studied these angles,[20] each patient is unique, and individualized bone tunnels need to be developed based on fluoroscopy. In conjunction with the high variability in the convexity of the distal femoral physis, simply adjusting the entry point of the parallel screw more distally and anteriorly is not an adequate solution to the risk of physeal injury.[10] Furthermore, it is worth emphasizing that even a slight deviation in the insertion point on the lateral radiograph may result in a significant deviation in the exit needle position on the anterior radiograph.[10]

Nowadays, the development and clinical application of orthopaedic robots may provide a more convenient and safe way to solve these problems. The aim of this study was to introduce robot-assisted MPFL femoral tunnel preparation and evaluate its clinical efficacy. Furthermore, during the surgery, the distance between the Schoettle point and the medial distal femoral physis, along with the simulated angle range of the bone tunnel and the optimal angle, was recorded in the robot-assisted group using an intraoperative 3-dimensional (3D) navigation system. To the best of our knowledge, robot-assisted individualized MPFL reconstruction on skeletally immature patients has not been reported so far in the literature.

METHODS

From June 2018 to August 2022, 76 skeletally immature patients with recurrent patellar dislocation were included. There were 31 males and 45 female patients. The study protocol was approved by the Ethics Committee of Honghui

‡Address correspondence to Liang Zhang, MD, Sports Medicine Center, Honghui Hospital, Xi'an Jiaotong University, No. 555 Friendship East Road, Beilin District, Xi'an, Shaanxi 710054, China (email: zlsports1981@163.com); Jiang Zheng, MD, Sports Medicine Center, Honghui Hospital, Xi'an Jiaotong University, No. 555 Friendship East Road, Beilin District, Xi'an, Shaanxi 710054, China (email: xymade369@163.com).

*Sports Medicine Center, Honghui Hospital, Xi'an Jiaotong University, Xi'an, Shaanxi, China.

†Department of Imaging, The Hospital of Xidian Group, Xi'an, Shaanxi, China.

Q.L., C.L., Z.Z., and J.L. contributed equally to this work.

Hospital, Xi'an Jiaotong University, and all patients signed a written informed consent form to have their information disclosed in this report. There were 42 patients who underwent robot-assisted physeal-sparing MPFL reconstruction (robot group) and 34 patients who underwent adductor magnus sling MPFL reconstruction (traditional group). Preoperative images were examined to determine the growth plate status, lower extremity alignment, tibial tubercle–trochlear groove (TT-TG) distance, Q-angle, and femoral neck anteversion. The mean operative time for both groups, the duration of each major procedure in the robot group, and the time taken to return to sport for each group were recorded. Exclusion criteria were previous knee surgery, revision surgery, TT-TG distance >22 mm, genu valgum >10°, femoral neck anteversion >25°, and severe rotation of the affected lower extremity >30°. The clinical results were evaluated using preoperative and postoperative International Knee Documentation Committee (IKDC) scores, Kujala scores, and imaging assessments, including limb length discrepancy on standing radiographs and patellar tilt angle. Patellar tracking was assessed both passively and actively, by observing the position of the patella in relation to the trochlea during knee flexion and extension.

Robot Group: Robot-Assisted Physeal-Sparing MPFL Reconstruction

After general anesthesia was administered, patients were placed supine on a radiolucent table, and the semitendinosus tendon was harvested. A 1.5 cm– to 2 cm–long, 2 mm–deep bone groove was created in the upper one-third of the superomedial aspect of the patella. Two anchors were placed individually to secure the middle portion of the semitendinosus tendon. A guide needle was inserted into the distal femur, and the tracer from the surgical robot TiRobot (TINAVI Medical Technologies Co, Ltd) was installed. Intraoperative images were captured using the O-arm (Medtronic Navigation Inc) and subsequently transferred to the robot workstation. The Schoettle point[21] was initially identified in the perfect lateral view using the image analysis system. A preliminary bone tunnel was then designed within the epiphysis, distal to the epiphyseal plate, extending from the Schoettle point to the lateral wall of the femoral lateral condyle. This design aimed to avoid the epiphyseal area, intercondylar notch, and lateral condylar cartilage surface, as observed in the image analysis system. Then, the distance between the Schoettle point and the medial physis, as well as the simulated angle range of the bone tunnel, was recorded in the robot-assisted group using an intraoperative 3D navigation system (Figure 1D). Finally, the relative median angle was selected from the simulated angle range to prepare the bone tunnel. The optical tracking system monitored the movement path of the manipulator and verified whether there were any deviations. If any deviations were detected, the system automatically compensated to ensure the accuracy of the guide pin's placement location. Subsequently, a 6-mm drill was used for the medial condyle

and a 4.5-mm drill for the lateral condyle to create the bone tunnel, after determining the isometric length of the ligament through flexion and extension of the knee joint. Finally, the semitendinosus tendon was secured at the Schoettle point using an interference screw. After reconstructing the MPFL, arthroscopy was performed to assess whether the lateral patellar retinaculum was too tight, especially after knee flexion. If necessary, the lateral retinaculum could be released. A typical case is shown in Figure 1.

Intraoperative Measurement of the Range of Angles and the Optimum Angle

During the operation, a real-time 3D computed tomography imaging navigation simulation system was utilized to identify the angle range that would not affect the epiphyseal area, intercondylar fossa, or lateral condylar cartilage surface of the femur, as well as to recommend the optimal angle. The specific approach is illustrated in Figure 2.

Traditional Group: Adductor Magnus Sling MPFL Reconstruction

The fixation of the patellar semitendinosus tendon was the same as that in the robot group. The femoral side was anchored by suspending the insertion of the adductor magnus tendon. The 2 ends of the semitendinosus tendon were looped around the insertion point of the adductor magnus tendon, folded at 30° of knee flexion, and then sutured in place. The principle of lateral retinaculum release is the same as that in the robot group. The technique is shown in Figure 3.

Statistical Analysis

Statistical analysis was performed using SPSS Version 20.0 software (IBM Corp). The normality of measurement data was examined to ensure they followed a normal distribution. These data are presented as mean ± standard deviation. Comparisons between groups were conducted using independent-samples t tests. Categorical data (such as sex) are presented as frequency (percentage), and comparisons between groups were performed using chi-square tests. A statistically significant difference was defined as a P value <.05

RESULTS

The mean age of the patients was 13.3 years (range, 10-16 years). All patients returned for follow-up, at a mean of 39.7 ± 9.8 months after surgery (Table 1). The mean operative time was 85.0 ± 16.3 minutes in the robot group. This included approximately 10 minutes for installation of the relevant navigation system and aseptic placement, about 5 minutes for image acquisition and uploading to the computer, around 10 minutes for planning the bone canal, approximately 5 minutes for refluoroscopic verification,
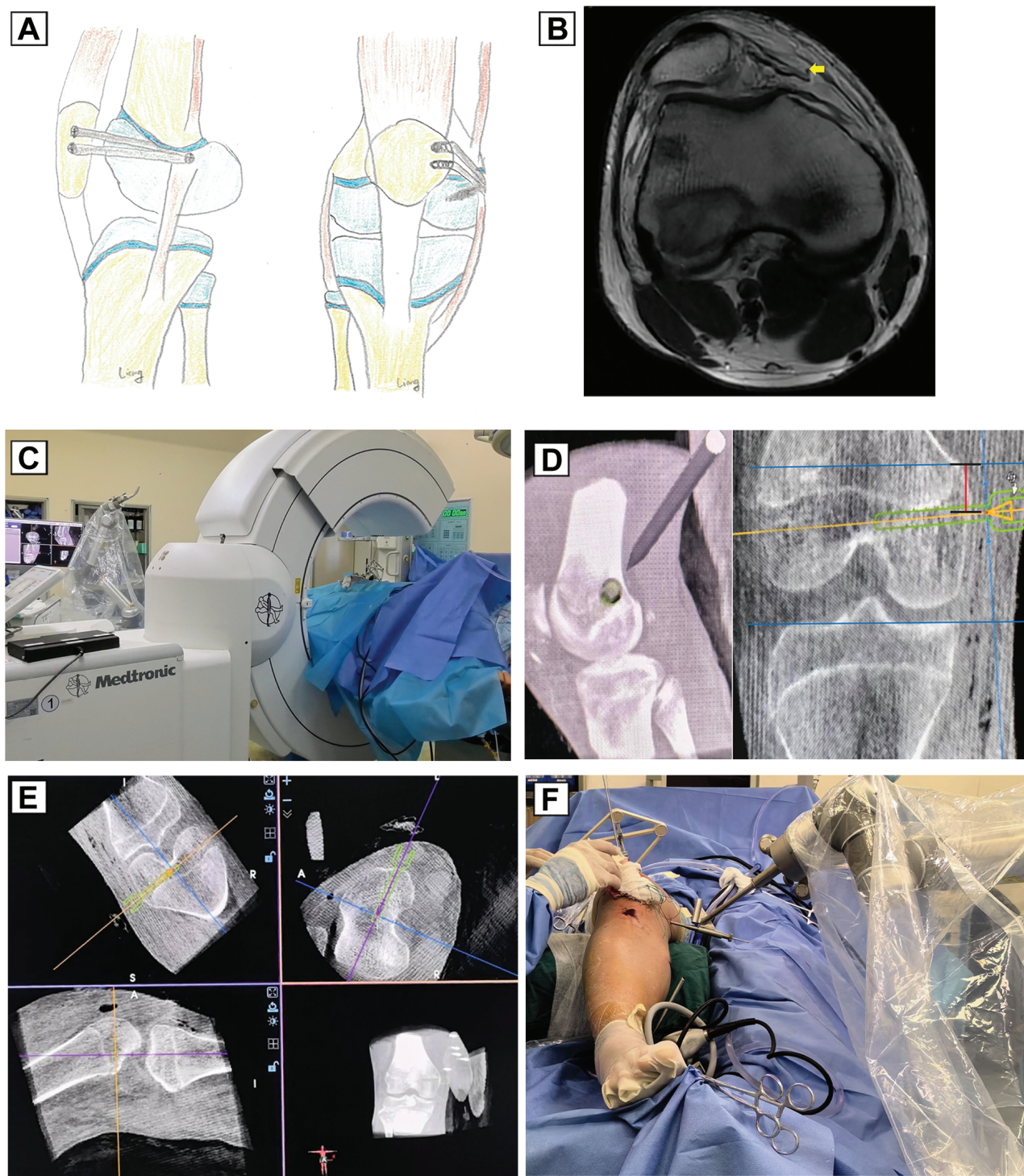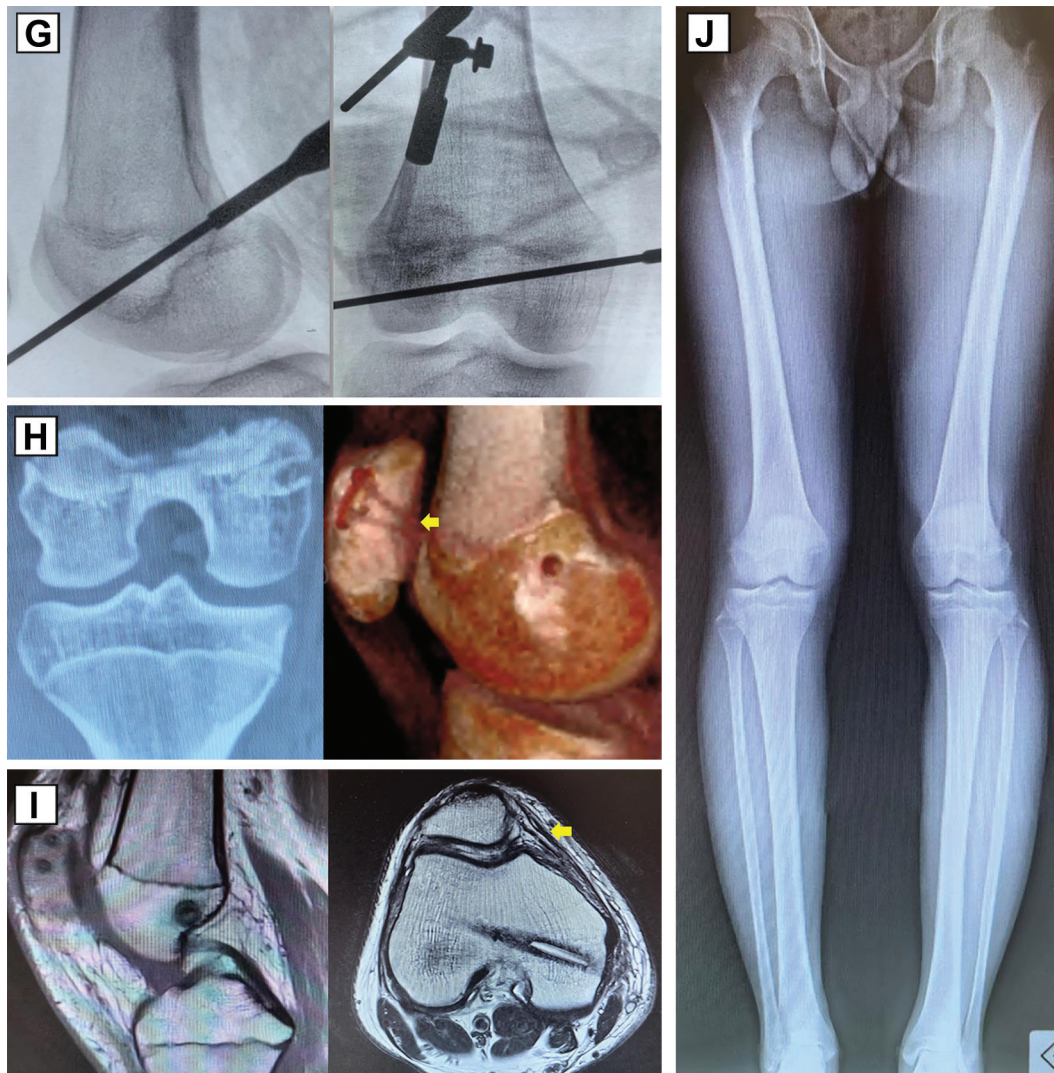
Figure 1. (continued)

Figure 1. A 13-year-old male patient with recurrent patellar dislocation underwent robot-assisted medial patellofemoral ligament (MPFL) reconstruction. (A) Schematic diagram of the physeal-sparing MPFL anatomic reconstruction. (B) Preoperative magnetic resonance imaging (MRI) revealed patellar subluxation and a ruptured MPFL (yellow arrow). (C) The intraoperative O-arm navigation system was utilized to collect images, which were then transmitted to the surgical robot. (D) The MPFL femoral tunnel was planned within the distal epiphysis according to the Schoettle point, avoiding the epiphyseal plate, and the vertical distance (red line) between the Schoettle point and the epiphysis was measured on the coronal plane of the femur. (E) Intraoperative 3-dimensional simulation navigation was used to determine the safe range and optimal angle. (F) The robotic arm assisted in the implantation of the guide needle. (G) Intraoperative lateral and anteroposterior fluoroscopic images confirmed that the guide pin was positioned within the distal femoral epiphysis. (H) Postoperative computed tomography showed the relationship between the bone tunnel, epiphyseal plate, Schoettle point, and reconstructed MPFL (yellow arrow). (I) MRI performed 32 months after surgery showed the implants in the epiphysis and patella, a well-aligned patellofemoral joint, and the reconstructed MPFL (yellow arrow). (J) A radiograph obtained 36 months after surgery indicated that the limbs were in good alignment with no signs of growth disturbance.

and roughly 30 minutes for bone canal preparation and MPFL reconstruction. The mean operative time in the traditional group was 37.7 ± 10.7 minutes, which showed a significant difference compared with the robot group ($P < .001$). The mean time required to return to sport (jogging) in the robot group was 14.6 ± 3.8 weeks, while in the traditional group it was 15.7 ± 4.0 weeks, with no significant difference ($P = .240$).

Additional procedures performed during MPFL reconstruction are recorded in Table 2. The Schoettle point was distal to the medial distal femoral physis in all cases, with a mean distance of 6.48 ± 1.78 mm from Schoettle
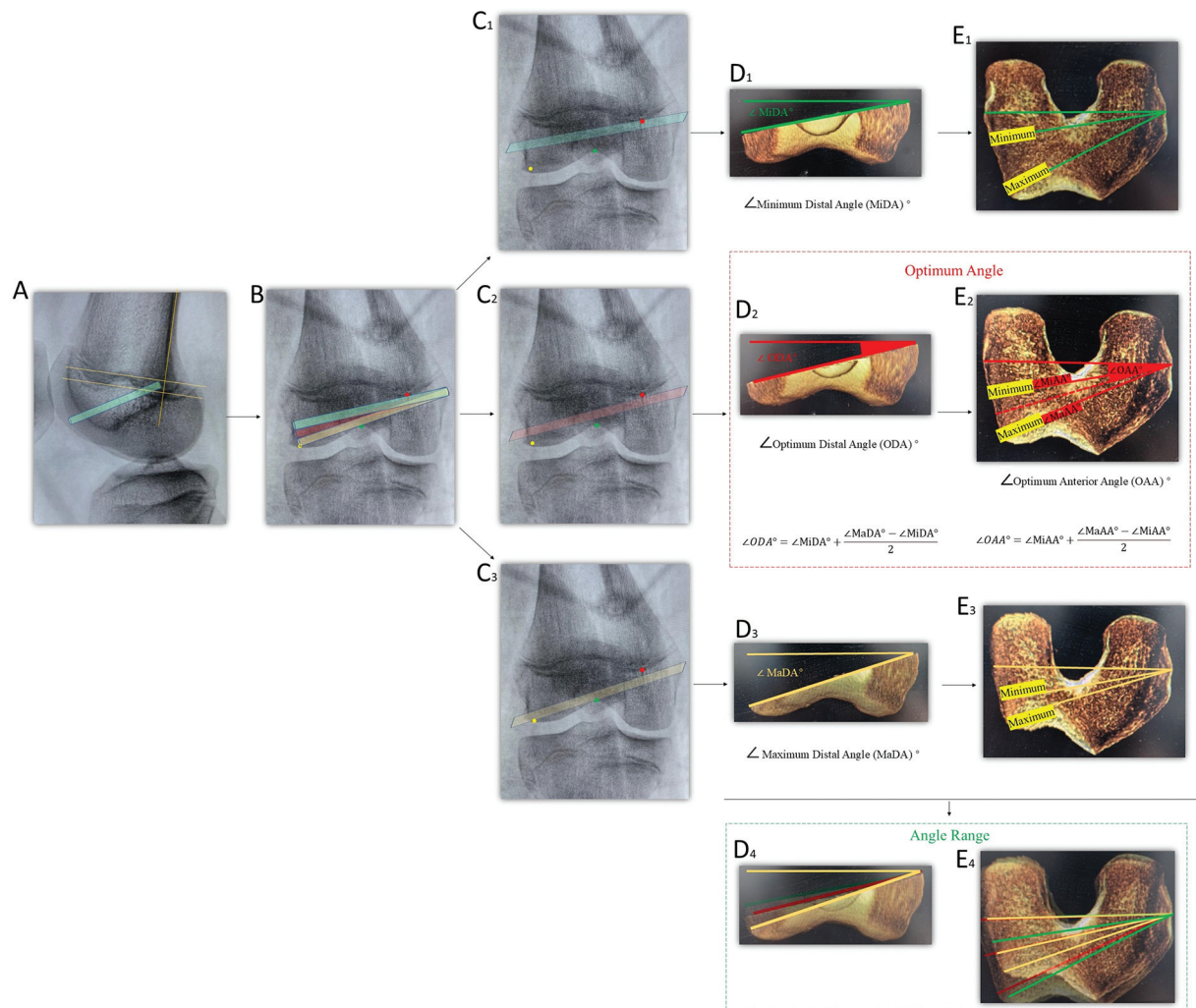
Figure 2. Schematic diagram of the optimum angle and the range of angles for the medial patellofemoral ligament femoral bone tunnel using an intraoperative 3-dimensional (3D) navigation system. (A) Planning the bone tunnel toward the distal femur according to the Schoettle point as observed in the lateral view. (B) The green bone tunnel is nearest to the lowest point (red dot) of the medial epiphyseal plate section, while the yellow bone tunnel is nearest to both the intercondylar fossa (green dot) and the lateral condylar cartilage surface of the femur (yellow dot). The red bone tunnel is located at the center of the 2 bone tunnels. (C) Three angles and oblique sections were established based on the 3 distinct bone tunnels. (D) The minimum, maximum, and optimum distal angles were recorded after safety, which was assessed through 3D simulation ($\angle ODA° = \angle MiDA° + \frac{\angle MaDA° - \angle MiDA°}{2}$). (E) After determining the 3 distal angles, corresponding oblique sections were constructed, and the maximum and minimum anterior angles were simulated within the robot system. The optimum anterior angle ($\angle OAA° = \angle MiAA° + \frac{\angle MaAA° - \angle MiAA°}{2}$) is identified on the oblique section corresponding to the best distal angle (red box), while the angle range indicates the minimum and maximum angles after superposition (green box). MaAA, maximum anterior angle; MaDA, maximum distal angle; MiAA, minimum anterior angle; MiDA, minimum distal angle; OAA, optimum anterior angle; ODA, optimum distal angle.

points to the medial distal femoral physis. The angle range of the bone tunnel was achieved by targeting a mean of 8.6° ± 2.5° to 23.4° ± 5.1° anteriorly and 10.9° ± 3.1° to 17.8° ± 4.4° distally, with the optimal angles being 14.6° ± 2.3° anteriorly and 13.5° ± 2.6° distally. No patients experienced recurrent patellar instability after surgery; however, the functional scores in the robot-assisted group were slightly higher than those in the traditional adductor magnus sling group at the last follow-up ($P < .05$). All the patients have normal patellar tracking, except for 3 patients (8.8%) in adductor magnus sling group. The robot group exhibited higher IKDC and Kujala scores compared with the traditional group at the last follow-up ($P < .05$) (Table 3). Magnetic resonance imaging scans performed
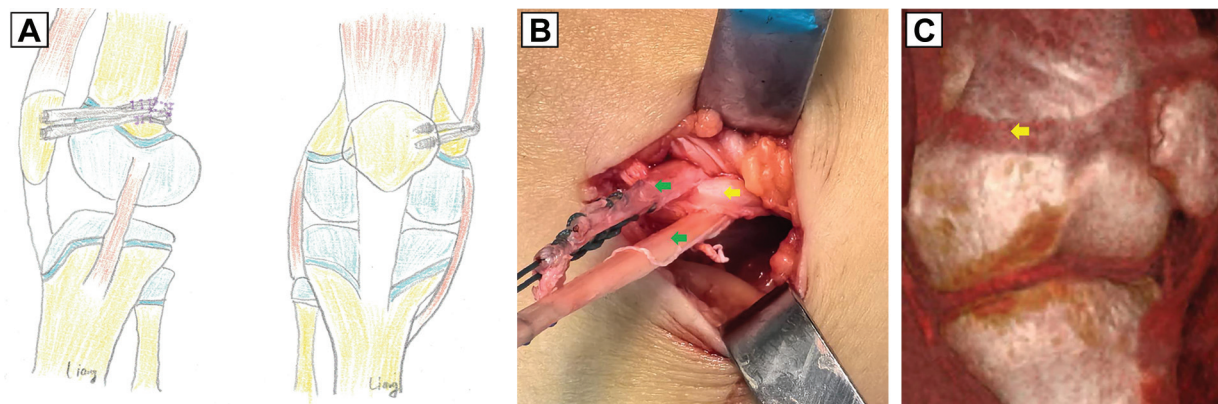
Figure 3. A 12-year-old female patient with recurrent patellar dislocation underwent the adductor magnus sling technique for medial patellofemoral ligament (MPFL) reconstruction. (A) Schematic diagram of the adductor magnus sling technique. (B) The 2 ends of the semitendinosus (green arrows) encircled the adductor magnus (yellow arrow) from front to back and from back to front, respectively, and were sutured and suspended to the adductor magnus tubercle. (C) Three-dimensional computed tomography reconstruction conducted 4 years after surgery showed a reconstructed MPFL (yellow arrow) and a closed epiphysis.

TABLE 1
Comparison of Baseline Data Between the 2 Groups[a]

	Robot Group	Traditional Group	P Value
No. of cases	42	34	
Sex, male/female	17 (40.5)/25 (59.5)	14 (41.2)/20(58.9)	.951
Age, y	13.2 ± 2.1	12.3 ± 2.6	.113
IKDC score	29.3 ± 5.9	26.7 ± 8.0	.102
Lysholm score	32.3 ± 6.4	35.1 ± 7.2	.073
Patellar tilt angle, deg	28.0 ± 4.5	26.5 ± 5.0	.171
TT-TG distance, mm	18.6 ± 3.8	19.0 ± 3.1	.568
Q-angle, deg	14.3 ± 3.2	13.2 ± 3.6	.170
Osteochondral free body	10 (23.8)	8 (23.5)	.951
Beighton score	3.2 ± 2.1	2.8 ± 2.3	.469

[a]Results are presented as n (%) or mean ± SD unless otherwise indicated. IKDC, International Knee Documentation Committee; TT-TG, tibial tubercle–trochlear groove.

TABLE 2
Additional Procedures Performed During MPFL Reconstruction[a]

Concomitant Procedure	Robot Group	Traditional Group	P Value
Loose-body removal	4 (9.5)	3 (8.8)	>.999
Fixation of osteochondral fragment	6 (14.3)	5 (14.7)	>.999
Lateral retinacular release	22 (52.4)	17 (50.0)	.836
Partial meniscectomy	3 (7.1)	3 (8.8)	>.999

[a]Results are presented as n (%). MPFL, medial patellofemoral ligament.

TABLE 3
Comparison of Postoperative Index in the 2 Groups[a]

	Postoperative Index at Last Follow-up		
	Robot Group	Traditional Group	P Value
IKDC score	93.2 ± 6.2	86.1 ± 7.9[b]	<.001
Lysholm score	90.0 ± 8.1	85.9 ± 7.3[b]	.026
Kujala score	87.8 ± 6.8	83.0 ± 8.8[b]	.009
PTA, deg	13.7 ± 2.6	14.4 ± 2.5	.218

[a]IKDC, International Knee Documentation Committee; PTA, patellar tilt angle.
[b]$P < .05$ compared with the robot group.

after operation did not show any signs of dysfunction of the reconstructed MPFL or cartilage degeneration. None of the patients in the robot group exhibited malalignment of the lower extremity or any evidence of physeal invasion.

DISCUSSION

The most important finding of the present study is that robot-assisted individualized MPFL reconstruction can be

safely performed in patients with open epiphyses. The intraoperative robotic navigation system confirmed that individualized anatomic reconstruction of the MPFL using a forward distal oblique bone tunnel is both safe and effective, demonstrating better clinical outcomes compared with the adductor magnus sling technique. The mean distance from Schoettle points to the medial distal femoral physis was 6.48 ± 1.78 mm, and the optimal angles for the bone tunnel were achieved by targeting 14.6° anteriorly and 13.5° distally. Several studies have described the osseous and soft tissue landmarks for femoral insertion of the MPFL in relation to the adductor tubercle, medial epicondyle, and osseous groove around these landmarks.[9] However, intraoperative identification of these landmarks was sometimes difficult due to scar formation, tissue swelling, and, more importantly, the femoral epiphysis is almost impossible to locate by direct palpation. In addition, it was reported that all femoral insertion sites were identified within a 7-mm radius around the center of the Schoettle point using fluoroscopy, while only 52% of femoral insertion sites identified by palpation were within this radius.[15] Therefore, in the present study, the Schoettle point was selected during the operation, and the femoral bone tunnel was customized by aligning it with the epiphysis of each patient.

In the present study, the Schoettle point appears directly in line with the physis on a true lateral radiograph, whereas the physis lies proximal to the Schoettle point on an anteroposterior radiograph. This is because the concave curvature of the distal femoral physis may be misleading for determining the relationship on the lateral radiograph.[19] Uppstrom et al[26] reported that placing the femoral screw distal to the femoral physis is an effective method for avoiding physeal injury with fluoroscopic guidance. The median distances from the physis to the socket at the aperture and distal end of the femoral socket were 5.9 mm (range, 1.9-12 mm) and 7.1 mm (range, 1.3-12.4 mm), respectively. Shea et al[23] reported that the insertion of the MPFL was located 2 to 5 mm proximal to the distal femoral physis, based on an indirect radiographic study utilizing lateral radiographs. Kepler et al[14] as well as Balcarek et al[2] have shown that the zone of insertion is just distal to the distal femoral physis. In contrast to their findings, direct intraoperative 3D navigation in the present study may facilitate more individualized anatomic reconstruction. The intraoperative robotic navigation system confirmed that the Schoettle point can be safely positioned in patients with open epiphyses. All Schoettle points were found to be positioned below the medial distal femoral physis, with a mean distance of 6.48 ± 1.78 mm from the Schoettle points to the medial distal femoral physis. This proximity facilitates relatively easy preparation of the femoral tunnel.

More importantly, in addition to determining the Schoettle point, the angle of the bone canal must be accurately taken into account. Nguyen et al[20] reported that angling the drill appropriately at 15° to 20° both distally and anteriorly minimizes damage to the physis, notch, and distal femoral cartilage. Irarrázaval et al[13] reported that the ideal femoral tunnel orientation, avoiding physeal

damage and breaching of the intercondylar notch, was achieved when aiming 30° to 40° distal and 5° to 35° anterior. In contrast, we reported a smaller range of angles, mainly because we utilized a bone canal through the medial and lateral condyles of the femur, which facilitates tendon implantation and ensures safe interfacial screw fixation. To the best of our knowledge, there are no similar reports of this angle in the literature. Based on our experience with surgical navigation, the closer the Schoettle point is to the epiphysis, the greater the distal angulation that may be required to avoid the epiphysis. At the same time, this means that there is an increased risk of injury to the intercondylar notch and femoral cartilage, and the forward angulation needs to be carefully designed to avoid injury to the notch and cartilage. Obviously, these angles vary for each child, so in each case, it is necessary for the robot to plan the position and orientation in advance.

Furthermore, although Schoettle points were distal to the physis in all patients in this study, this does not imply that the angle of the screw can be placed arbitrarily within the distal epiphysis, as the diameter of the screw must be considered. The heat generated by the spinning drill and the bony compression from the fixation should also be considered. Computer navigation can simultaneously consider all these factors and assist in planning the ideal angle. Therefore, the maximum anterior and distal inclinations that did not affect the epiphyseal, intercondylar fossa, and lateral condylar cartilage surfaces were individually recorded during the operation. The results indicated that the angle range of the bone tunnel was achieved by targeting a mean of 8.6° to 23.4° anteriorly and 10.9° to 17.8° distally, with the optimal angles being 14.6° anteriorly and 13.5° distally. We also recommend maintaining a distance of at least 1 mm between the outer wall of the bone tunnel and the lowest point of the medial epiphyseal plate section.

Additionally, according to the literature, the distance between the original insertion of the MPFL and the physis may decrease or increase as skeletal maturity is approached. Some authors have suggested that the MPFL origin begins distal to the physis and moves proximally with age, while some authors have found a statistically significant increase in the distance between the MPFL and the physis with advancing age.[10] As no consensus has been reached, utilizing computer simulation navigation for individualized bone tunnel preparation may be considered one of the optimal approaches.

In the study by Weeks et al,[27] anteroposterior fluoroscopic imaging was first used to confirm that the starting point was located distal to the femoral physis, followed by the use of lateral fluoroscopic imaging to guide the positioning of the guide wire. In the current study, this sequence differs from the previously described procedure. We first identified the Schoettle point using lateral fluoroscopic imaging and then adjusted its position on anteroposterior fluoroscopic imaging to accurately locate the Schoettle point without affecting the epiphysis or its nearest point. It should be noted that on lateral fluoroscopic imaging, the femoral insertion point may falsely appear to be proximal to the physis because of the nonlinear structure of the distal femoral growth plate. With the help of the

intraoperative robotic navigation system, this positioning process is streamlined through simulated positioning, minimizing the need for repeated punctures.

Uppstrom et al[26] reported the outcomes of isolated MPFL reconstruction using a physeal-sparing technique with a follow-up of 2.2 years. Among 5 patients (9.3%), recurrent patellar instability was observed, with 3 patients (5.6%) requiring subsequent tibial tubercle osteotomy or revision MPFL reconstruction. In the present study, no recurrent patellar instability was observed in the robot group. This may be attributed to the use of a longer bone tunnel through the internal and external condyles of the femur, which is more conducive to tendon fixation and tendon-bone healing.

In contrast, the adductor magnus sling technique was used in the traditional group, where a free graft is wrapped around the adductor magnus tendon. Patellar maltracking in the present study may be caused by the following reasons: (1) The adductor sling becomes tighter in flexion, potentially leading to graft stretching or even failure.[4] (2) The fixation strength of the adductor sling is not as good as that of a screw, as screw fixation involves tendon-bone healing, while the adductor sling involves soft tissue healing. (3) In comparison with anatomic MPFL reconstruction, nonanatomic MPFL techniques, such as the adductor tendon loop method, may place excessive stress on the medial patellofemoral joint, potentially resulting in early failure. (4) Although only minimal changes in patellofemoral kinematics and contact mechanics occurred at the extremes of flexion, a more distal fixation position is biomechanically advantageous over the more proximal fixation sites.[3] Overall, although both surgical methods significantly improved patellar stability and achieved favorable clinical outcomes, our final follow-up revealed that the functional IKDC and Kujala scores in the robot group were significantly higher than those in the traditional group. This difference may be attributed to the superior patellofemoral relationship achieved by the robot group during anatomic reconstruction, in contrast to the nonanatomic nature of the femoral attachment. Additionally, a graft placed in the epiphysis is likely to maintain a more stable position in a growing child.

Limitations

Robotic surgery tends to be relatively time-consuming, and there is a significant variation in the recorded operating times. The shorter operative times observed in the later stages may be attributed to the staff and surgeons becoming more familiar with the procedures. In addition, the selection of the control group is not optimal, and we plan to compare the medium- and long-term efficacy across additional groups in the future. This study is beneficial for surgeons in the early stages of their careers or those with a low volume of MPFL reconstruction practices in skeletally immature patients; however, for physicians with extensive experience in epiphyseal-sparing techniques, they can rely on their own expertise to perform such procedures.

CONCLUSION

Despite the presence of open growth plates, surgical treatment for patellar instability in skeletally immature patients can be performed safely. The intraoperative robotic navigation system confirmed that the Schoettle point can be safely positioned in patients with open epiphyses. The Schoettle points were all located below the medial distal femoral physis, with a mean distance of 6.48 ± 1.78 mm from Schoettle points to the medial distal femoral physis. The angle range of the bone tunnel was achieved by targeting a mean of 8.6° to 23.4° anteriorly and 10.9° to 17.8° distally, with the optimal angles being 14.6° anteriorly and 13.5° distally. The robot-assisted design of individualized anatomic reconstruction of the MPFL using a forward distal oblique bone tunnel is safe, accurate, and effective in patients with unclosed epiphyses, demonstrating good clinical outcomes. We recommend this surgical technique for symptomatic children and adolescents experiencing recurrent patellar dislocation.

REFERENCES

1. Andrish J. Surgical options for patellar stabilization in the skeletally immature patient. *Sports Med Arthrosc Rev*. 2017;25(2):100-104. doi:10.1097/JSA.0000000000000145
2. Balcarek P, Ammon J, Frosch S, et al. Magnetic resonance imaging characteristics of the medial patellofemoral ligament lesion in acute lateral patellar dislocations considering trochlear dysplasia, patella alta, and tibial tuberosity-trochlear groove distance. *Arthroscopy*. 2010;26:926-935.
3. Bicos J, Fulkerson JP, Amis A. Current concepts review: the medial patellofemoral ligament. *Am J Sports Med*. 2007;35(3):484-492. doi:10.1177/0363546507299237
4. Black SR, Meyers KN, Nguyen JT, et al. Comparison of ligament isometry and patellofemoral contact pressures for medial patellofemoral ligament reconstruction techniques in skeletally immature patients. *Am J Sports Med*. 2020;48(14):3557-3565. doi:10.1177/0363546520966609
5. Bouras T, Edmond U, Brown A, Gallacher P, Barnett A. Isolated medial patellofemoral ligament reconstruction significantly improved quality of life in patients with recurrent patella dislocation. *Knee Surg Sports Traumatol Arthrosc*. 2019;27(11):3513-3517. doi:10.1007/s00167-019-05447-w
6. Chen J, Han K, Jiang J, et al. Radiographic reference points do not ensure anatomic femoral fixation sites in medial patellofemoral ligament reconstruction: a quantified anatomic localization method based on the saddle sulcus. *Am J Sports Med*. 2021;49(2):435-441. doi:10.1177/0363546520972420
7. Chotel F, Bérard J, Raux S. Patellar instability in children and adolescents. *Orthop Traumatol Surg Res*. 2014;100(1 suppl):S125-S137. doi:10.1016/j.otsr.2013.06.014
8. Farrow LD, Alentado VJ, Abdulnabi Z, Gilmore A, Liu RW. The relationship of the medial patellofemoral ligament attachment to the distal femoral physis. *Am J Sports Med*. 2014;42(9):2214-2218. doi:10.1177/0363546514539917
9. Fujino K, Tajima G, Yan J, et al. Morphology of the femoral insertion site of the medial patellofemoral ligament. *Knee Surg Sports Traumatol Arthrosc*. 2015;23(4):998-1003. doi:10.1007/s00167-013-2797-0
10. Greenrod W, Cox J, Astori I, Baulch J, Williams J. A magnetic resonance imaging study of the significance of the distal femoral physis during medial patellofemoral ligament reconstruction. *Orthop J Sports Med*. 2013;1(4):2325967113502638. doi:10.1177/2325967113502638

11. Hennrikus W, Pylawka T. Patellofemoral instability in skeletally immature athletes. *J Bone Joint Surg Am*. 2013;95(2):176-183.

12. Hensler D, Sillanpaa PJ, Schoettle PB. Medial patellofemoral ligament: anatomy, injury and treatment in the adolescent knee. *Curr Opin Pediatr*. 2014;26(1):70-78. doi:10.1097/MOP.00000000 00000055

13. Irarrázaval S, Besa P, Fernández F, et al. Anterior and distal tunnel orientation for anatomic reconstruction of the medial patellofemoral ligament is safer in patients with open growth plates. *Knee Surg Sports Traumatol Arthrosc*. 2021;29(6):1822-1829. doi:10.1007/ s00167-020-06229-5

14. Kepler CK, Bogner EA, Hammoud S, Malcolmson G, Potter HG, Green DW. Zone of injury of the medial patellofemoral ligament after acute patellar dislocation in children and adolescents. *Am J Sports Med*. 2011;39:1444-1449.

15. Koenen P, Shafizadeh S, Pfeiffer TR, et al. Intraoperative fluoroscopy during MPFL reconstruction improves the accuracy of the femoral tunnel position. *Knee Surg Sports Traumatol Arthrosc*. 2018;26(12): 3547-3552. doi:10.1007/s00167-018-4983-6

16. LaPrade RF, Engebretsen AH, Ly TV, Johansen S, Wentorf FA, Engebretsen L. The anatomy of the medial part of the knee. *J Bone Joint Surg Am*. 2007;89(9):2000-2010. doi:10.2106/JBJS.F.01176

17. Melegari TM, Parks BG, Matthews LS. Patellofemoral contact area and pressure after medial patellofemoral ligament reconstruction. *Am J Sports Med*. 2008;36(4):747-752. doi:10.1177/036354650 8314410

18. Nelitz M, Dornacher D, Dreyhaupt J, Reichel H, Lippacher S. The relation of the distal femoral physis and the medial patellofemoral ligament. *Knee Surg Sports Traumatol Arthrosc*. 2011;19(12):2067-2071. doi:10.1007/s00167-011-1548-3

19. Nelitz M, Reichel H, Dornacher D, Lippacher S. Anatomic reconstruction of the medial patellofemoral ligament in children with open growth plates. *Arch Orthop Trauma Surg*. 2012;132(11):1647-1651. doi:10.1007/s00402-012-1593-5

20. Nguyen CV, Farrow LD, Liu RW, Gilmore A. Safe drilling paths in the distal femoral epiphysis for pediatric medial patellofemoral ligament reconstruction. *Am J Sports Med*. 2017;45(5):1085-1089. doi:10. 1177/0363546516677795

21. Schöttle PB, Fucentese SF, Romero J. Clinical and radiological outcome of medial patellofemoral ligament reconstruction with a semitendinosus autograft for patella instability. *Knee Surg Sports Traumatol Arthrosc*. 2005;13(7):516-521. doi:10.1007/s00167-005-0659-0

22. Schöttle PB, Schmeling A, Rosenstiel N, Weiler A. Radiographic landmarks for femoral tunnel placement in medial patellofemoral ligament reconstruction. *Am J Sports Med*. 2007;35(5):801-804. doi:10. 1177/0363546506296415

23. Shea KG, Grimm NL, Belzer J, Burks RT, Pfeiffer R. The relation of the femoral physis and the medial patellofemoral ligament. *Arthroscopy*. 2010;26:1083-1087.

24. Shea KG, Polousky JD, Jacobs JC Jr, et al. The relationship of the femoral physis and the medial patellofemoral ligament in children: a cadaveric study. *J Pediatr Orthop*. 2014;34(8):808-813. doi:10. 1097/BPO.0000000000000165

25. Shea KG, Styhl AC, Jacobs JC Jr, et al. The relationship of the femoral physis and the medial patellofemoral ligament in children: a cadaveric study. *Am J Sports Med*. 2016;44(11):2833-2837. doi:10.1177/0363546516656366

26. Uppstrom TJ, Price M, Black S, Gausden E, Haskel J, Green DW. Medial patellofemoral ligament (MPFL) reconstruction technique using an epiphyseal femoral socket with fluoroscopic guidance helps avoid physeal injury in skeletally immature patients. *Knee Surg Sports Traumatol Arthrosc*. 2019;27(11):3536-3542. doi:10.1007/ s00167-019-05412-7

27. Weeks KD III, Fabricant PD, Ladenhauf HN, Green DW. Surgical options for patellar stabilization in the skeletally immature patient. *Sports Med Arthrosc Rev*. 2012;20(3):194-202.

28. Yercan HS, Erkan S, Okcu G, Ozalp RT. A novel technique for reconstruction of the medial patellofemoral ligament in skeletally immature patients. *Arch Orthop Trauma Surg*. 2011;131(8):1059-1065. doi:10. 1007/s00402-011-1305-6